Short-range order in Ni-Pt alloys

1995 J. Phys.: Condens. Matter 7 3203

(http://iopscience.iop.org/0953-8984/7/17/004)

J. Phys.: Condens. Matter 7 (1995) 3203–3209. Printed in the UK

Short-range order in Ni–Pt alloys

Dilip Kumar Saha and Ken-ichi Ohshima
Institute of Applied Physics, University of Tsukuba, Tsukuba 305, Japan

Received 14 November 1994, in final form 23 January 1995

Abstract. Electron and x-ray diffraction patterns were taken from four different $Ni_{1-x}Pt_x$ alloys, with $x = 0.25, 0.35, 0.44$ and 0.50, to understand the existence and shape of the diffuse intensity, which gives us information about structural fluctuations. A peculiar shape of diffuse scattering has been observed at 1 0 0 and 1 1 0 and their equivalent positions in the patterns, the shape of the diffuse intensity at the 1 0 0 position changing with Pt content in the alloys. The shape of the diffuse intensity at the 1 0 0 position for the $x = 0.25$ alloy is rod-like, but the shape is nearly spherical for the $x = 0.50$ alloy. The x-ray diffuse scattering intensities were measured from the $x = 0.50$ single-crystal alloy at room temperature, and the Warren–Cowley short-range order parameters were determined after analysing the data. The correlation length has been deduced to be about 19 Å from estimating the inverse of the full width at half-maximum of the diffuse peak.

1. Introduction

In recent years, diffraction work has been done on disordered binary alloys to understand their structural fluctuations by analysing the short-range order (SRO) diffuse scattering intensity quantitatively. With the use of the thermodynamical treatment of SRO parameters, i.e. two-body correlation function, the origin of the atomic pair-interaction potential can be discussed. In particular, a portion of Fermi wavevector along a specific direction is seen on the SRO diffuse scattering intensity from some disordered alloys through the Krivoglaz–Moss theory (Krivoglaz 1969, Moss 1969). In general, the shape and position of diffuse maxima in the disordered state are independent of the type of ordered structure in the binary alloys. There are some remarkable experimental results in the disordered Cu–Pd and Cu–Pt alloy systems. Twofold and fourfold splittings of diffuse scattering in the disordered Cu–Pd alloys were observed at 1 0 0 and 1 1 0 and their equivalent positions, with the separation changing continuously with the composition (Ohshima and Watanabe 1973, Saha *et al* 1992), though two different ordered structures (Cu_3Au and CsCl types) exist in some of the composition range. On the other hand, extra diffuse maxima at $\frac{1}{2}\ \frac{1}{2}\ \frac{1}{2}$ and its equivalent positions were observed in addition to the composition-dependent split diffuse maxima in the disordered Cu–Pt alloys (Ohshima and Watanabe 1973, Saha and Ohshima 1993), in which three different ordered structures (Cu_3Pt, CuPt and $CuPt_3$) exist.

Short-range order in some Ni-based binary alloys has been studied: Ni–Cr, Ni–Mo and Ni–Fe (Kostorz 1983, Schönfeld *et al* 1994) and Ni–Al (Klaiber *et al* 1987). But there are no reports on the diffuse scattering study of Ni–Pt alloys, though characteristic physical properties have already been reported as follows. Dahmani *et al* (1985) have measured the temperature dependence of atomic relaxation times for both the ordered and disordered states in the Ni–Pt alloys. They have observed the important slowing-down effects in the vicinity of the order–disorder transition temperature, T_p. Cadeville *et al* (1986) have

0953-8984/95/173203+07$19.50

measured the relationship between the magnetism and randomness in Ni–Pt alloys. It was found that the value of the ferromagnetic–paramagnetic transition temperature, T_c, strongly depends on the heat treatment. Temperature T_c for the quenched specimen is higher than that for a sample that has undergone long annealing below T_p. They pointed out that such behaviour indicates the effect of ordering on the magnetic property. It is quite unknown whether the SRO diffuse intensity actually exists or not in the Ni–Pt alloy system. On the other hand, alloys of concentration from $x = 0.23$ up to about 0.35 and from $x = 0.56$ up to about 0.70 in $Ni_{1-x}Pt_x$ alloys show the $L1_2$-type ordered structure, and from $x = 0.41$ up to 0.53 alloys show the $L1_0$-type structure (layers of Ni and Pt atoms along the c axis) and $a = b \neq c$ below T_p (Cadeville *et al* 1986). But above T_p it shows the FCC structure in the whole composition range.

It is, therefore, our great interest to study the existence and shape of the SRO diffuse intensity in the disordered Ni–Pt alloys to understand structural fluctuations. In the Cu–Pt alloy system, an extra diffuse maximum was observed at $\frac{1}{2}\ \frac{1}{2}\ \frac{1}{2}$ and its equivalent position owing to the presence of $L1_1$-type layered structure. Ni is the neighbouring atom of Cu in the periodic table. If we replace Ni by Cu in the Cu–Pt alloy system, then what will happen in the diffuse intensity is also of interest (in the Ni–Pt alloy system, there is also a layered structure of $L1_0$ type). In the present paper we report the following experimental results: electron diffraction patterns from the three different concentrations of $x = 0.25$, 0.35 and 0.44 alloys, the SRO diffuse intensity from a single crystal with $x = 0.50$ using x-ray diffraction ad the structural characteristics of disordered Ni–Pt alloy after analysing the data.

2. Experimental procedure

Four polycrystalline samples were prepared by melting 99.999% pure Ni and 99.99% pure Pt using an arc melting furnace in an argon atmosphere. Subsequently, the alloys were remelted nine or ten times to homogenize the specimens. The sample ingots were rolled into thin sheets and strip-shaped samples were cut from the thin sheets for the x-ray Debye–Scherrer experiment. After heat treatment of the samples above T_p to remove strain, the lattice parameters of the quenched specimens in the disordered state were measured with an x-ray Debye–Scherrer camera using Cu Kα radiation. The specimen compositions were determined with an accuracy of ± 0.3 at.% by comparison with the lattice parameter (a_0) versus composition relation (Pearson 1958). The four compositions were determined as $x = 0.25$, 0.35, 0.44 and 0.50 in $Ni_{1-x}Pt_x$ alloys. The compositions of the alloys were selected in such a way that they will cover the two regions of different ordered structure. For the electron diffraction (ED) study, three samples of $x = 0.25$, 0.35 and 0.44 alloys, whose diameter and thickness were 3 mm and about 0.1 mm, respectively, were prepared using a punch machine. All the samples were annealed separately in evacuated silica tubes at 1000 °C for 4 days, 900 °C for 1 day and 800 °C for 10 days successively, and quenched by being dropped into iced water. Chemical etching was performed on the specimens at 75 °C in a hot water bath using 30% HNO_3, 10% HCl, 10% H_3PO_4 and 50% CH_3COOH solution. A JEM-200CX transmission electron microscope, operated at 200 kV and equipped with a specimen tilting device, was used and diffraction patterns for different orientations were obtained.

A single crystal of the $x = 0.50$ alloy was grown by the Bridgman technique in a high-purity alumina crucible at the Institute for Materials Research, Tohoku University, for the x-ray diffuse scattering experiment. A sample slice was cut parallel to a (2 1 0) plane from

the original single-crystal ingot, whose dimensions were $12 \times 10 \times 4$ mm^3. The slice was polished mechanically and etched chemically to remove the distorted surface layer. The etching solution was the same as that used for the ED samples. The sample was annealed in an evacuated silica tube at 1000 °C for 4 days, 900 °C for 1 day and 850 °C for 10 days successively to homogenize the specimen, and finally quenched by being dropped into iced water. The surface of the specimen was etched chemically again to remove the oxide layer.

The x-ray diffuse intensity measurement was performed at room temperature by using a four-circle goniometer attached to the rotor unit of an x-ray generator (Rigaku, RU-300). The incident beam, Cu Kα radiation, from a Cu target was monochromated by a singly-bent HOPG crystal. To remove Ni fluorescence from the sample, a HOPG analyser was used in front of the scintillation counter. The diffuse intensities were measured by scanning a volume of reciprocal space at intervals of $\Delta h_i = 1/40$ in terms of the distance between the 0 0 0 and 2 0 0 fundamental spots. Both the background and air scattering were estimated by irradiating a Si(3 1 1) single crystal with dimensions of $20 \times 15 \times 5$ mm^3 and were subtracted from the measured intensity. Primary beam power was estimated from the scattered intensity of polystyrene (C_8H_8) at $2\theta = 100°$. The procedure for the x-ray diffuse intensity analysis was the same as that used in the study of Cu–Pt alloy (Saha and Ohshima 1993). In particular, the intensity distribution due to SRO was separated using the Borie and Sparks (1971) method after removing the size-effect modulation, the Huang scattering and the thermal diffuse scattering from the total diffuse intensities.

3. Results and discussion

3.1. Electron diffraction study

The three electron diffraction patterns for the $x = 0.25$, 0.35 and 0.44 alloys are shown in figure 1(*a*)–(*c*), respectively, where the incident beam was parallel to the [0 0 1] direction. At 1 1 0 and its equivalent position, a similar pattern of diffuse intensity distribution was observed for all three alloys, where the shape of the diffuse intensity is almost spherical. But at 1 0 0 and its equivalent position, three different shapes of diffuse intensity distributions were observed for the three alloys. In figure 1(*a*), for the $x = 0.25$ alloy, the diffuse intensity distribution at 1 0 0 position is almost rod-like, with elliptical ends along the [0 1 0] direction. In a previous paper on Pd–Mn alloys (Saha *et al* 1994), we have observed similar trends of intensity distribution where the shape at the 1 0 0 position was rod-like and the shape at the 1 1 0 position was square-like. Figure 1(*b*), for the $x = 0.35$ alloy, shows different intensity distribution compared with that of the $x = 0.25$ alloy. In this case at 1 0 0 and its equivalent position, an elliptical pattern of diffuse intensity was observed. In figure 1(*c*), for the $x = 0.44$ alloy, the diffuse intensity distribution at 1 0 0 and its equivalent position is almost spherical.

Moss and Clapp (1968) applied the linearized approximation for the correlation function of a binary alloy to the experimental measurement of the diffuse scattering. In particular, the Cu–Au alloy system is a good example of this application. To realize the change in shape from being disc-like for Cu_3Au to nearly spherical for CuAu, diffuse intensity distributions are calculated by changing the values of pair-interaction potential ratios through the linearized intensity formula. They have understood that the change in shape from disc-like to nearly spherical is related to the increasing importance of the third-neighbour pair-interaction potential, V_3. In the case of the Ni–Pt alloy system, the same discussion is applicable because both the composition dependence of the shape of diffuse scattering and the alloy's phase diagram are similar to those for the Cu–Au alloy system. Therefore, the

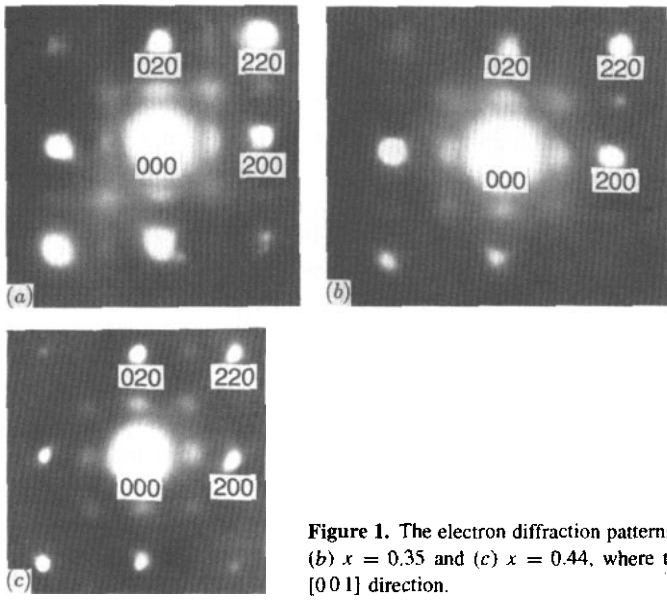

Figure 1. The electron diffraction patterns of $Ni_{1-x}Pt_x$ alloys for (*a*) $x = 0.25$, (*b*) $x = 0.35$ and (*c*) $x = 0.44$, where the incident beam was parallel to the [0 0 1] direction.

inclusion of the small value of V_3 was necessary in order to provide the nearly spherical diffuse pattern at the 1 0 0 position in figure 1(*c*).

3.2. X-ray diffraction study

In the ED study, we have observed that the shape of the diffuse intensity at the 1 0 0 position becomes more spherical with increasing Pt content in the alloys. Therefore, we have considered that the most appropriate alloy for the x-ray study is the stoichiometric ($x = 0.50$) one, in order to study the SRO diffuse intensity quantitatively. Figure 2(*a*) shows the SRO diffuse intensity distribution on the ($h\,k\,0$) reciprocal lattice plane in Laue units, where the contributions from size effect, temperature diffuse scattering plus Huang scattering, Compton scattering and air scattering have been subtracted. The corresponding bird's-eye view is shown in figure 2(*b*). The SRO diffuse intensity distribution has certainly been confirmed from this x-ray measurement. We have observed the spherical intensity distribution at the 1 1 0 position, which is the same as that for the ED study. On the other hand, we have deduced from the ED study that, for the $x = 0.50$ alloy, the diffuse intensity distribution at the 1 0 0 position would be more spherical. But we did not observe a spherical intensity distribution at the 1 0 0 position for the $x = 0.50$ alloy. The intensity distribution is still slightly elliptical. Further, we did not observe any extra diffuse intensity at $\frac{1}{2}\ \frac{1}{2}\ \frac{1}{2}$ and its equivalent position except the diffuse intensity at 1 0 0 and 1 1 0 and their equivalent positions. The correlation length is estimated to be about 19 Å from the inverse of the full width at half-maximum of the diffuse peak.

The Warren–Cowley SRO parameters, α_{lmn}, were determined from the experimental SRO diffuse intensities up to the 50th shell and are listed in table 1, where l, m and n are integers. The error was estimated to be less than ±5%. The first 40 SRO parameters versus distance, $r_{lmn} = (l^2 + m^2 + n^2)^{1/2}$, are plotted in figure 3. As seen in the figure, the sign of SRO parameters is positive for all even indices of l, m and n at least up to the 17th neighbour, and their magnitude decreases with increasing distance from the origin. On the other hand, the sign of SRO parameters is negative for mixed indices of l, m and n up to the 16th

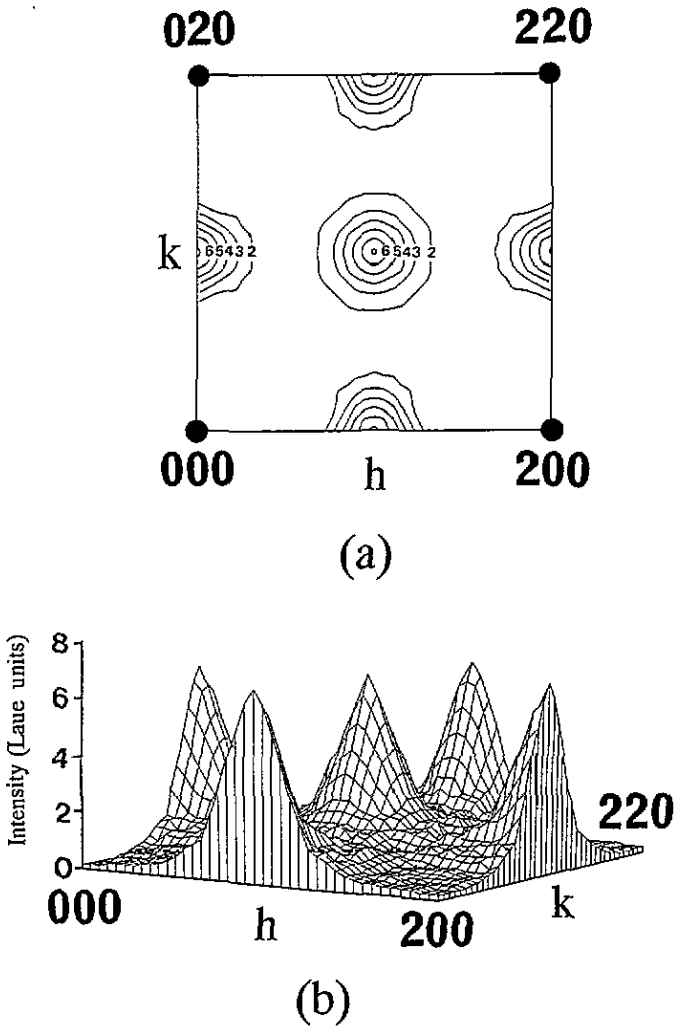

Figure 2. (*a*) The x-ray SRO diffuse scattering intensity distribution on the $(h\,k\,0)$ reciprocal lattice plane in Laue units for the $x = 0.50$ $Ni_{1-x}Pt_x$ alloy ($I_{min} = 2.0$, $\Delta I = 1.0$ and $I_{max} = 7.3$ Laue units) and (*b*) a bird's-eye view of (*a*).

neighbour. To find a structural characteristic of the disordered state, we have compared the sign and magnitude of SRO parameters for the NiPt alloy with the corresponding parameters for the perfectly ordered state of the stoichiometric $L1_0$-type layered structure. The value of the parameters for all even and mixed indices of l, m and n are 1 and $-1/3$, respectively. Thus, it is deduced that the local structure of the disordered state is similar to that for an ordered NiPt alloy.

To confirm the validity of SRO parameters thus determined experimentally, the diffuse intensity map was synthesized using all the 78 parameters. The diffuse intensity distribution thus reconstructed is almost the same as the observed one in figure 2.

Table 1. The SRO parameters α_{lmn} for the $x = 0.50$ $Ni_{1-x}Pt_x$ alloy determined from the Fourier transform to the SRO diffuse scattering intensities (N is the shell number).

N	$l\,m\,n$	α_{lmn}	N	$l\,m\,n$	α_{lmn}
	000	1.038	30	800	0.014
1	110	−0.126	31	554	−0.001
2	200	0.101		741	0.000
3	311	−0.026		811	−0.002
4	220	0.049	32	644	0.000
5	310	0.003		820	0.010
6	222	0.026	33	653	0.001
7	321	−0.002	34	660	−0.003
8	400	0.036		822	0.005
9	330	−0.020	35	743	0.000
	411	−0.004		750	0.000
10	420	0.020		831	−0.004
11	332	−0.009	36	662	0.003
12	422	0.019	37	752	−0.001
13	431	−0.006	38	840	−0.003
	510	−0.013	39	833	0.001
14	521	−0.005		910	−0.001
15	440	0.002	40	842	0.000
16	433	−0.004	41	655	0.000
	530	0.002		761	0.000
17	442	0.009		921	−0.001
	600	−0.005	42	664	0.002
18	532	−0.002	43	754	0.000
	611	−0.007		930	0.000
19	620	−0.004		851	0.002
20	541	0.000	44	763	−0.002
21	622	0.004		932	−0.001
22	631	0.001	45	844	0.000
23	444	0.000	46	770	0.001
24	543	−0.001		853	−0.002
	550	−0.003		941	0.000
	710	0.007	47	860	0.004
25	640	0.010		1000	−0.004
26	552	−0.001	48	772	0.002
	663	−0.001		1011	−0.009
	721	0.002	49	862	0.000
27	642	0.003		1020	−0.002
28	730	−0.004	50	943	0.002
29	651	−0.004		950	0.000
	732	−0.002			

4. Conclusion

The main aim of this paper was to study the existence and shape of diffuse intensity in Ni–Pt alloys. We have observed the composition dependence of diffuse intensity, where the shape of diffuse intensity changes with Pt content. The change in shape from disc-like to spherical can be explained with the use of the linearized correlation function. The present study has proved experimentally that the Ni–Pt alloys have strong SRO diffuse intensity above T_p, which had been proposed by Cadeville *et al* (1986). Another aim was to study the effect of Ni atoms instead of Cu atoms with Pt in the diffuse intensity. We did not observe any extra diffuse intensity like Cu–Pt alloys at $\frac{1}{2}\ \frac{1}{2}\ \frac{1}{2}$ position, though both the

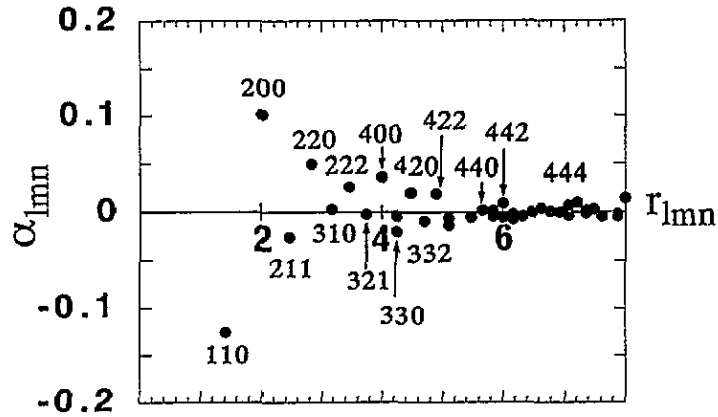

Figure 3. The first 40 SRO parameters α_{lmn} versus distance r_{lmn} for the $x = 0.50$ $Ni_{1-x}Pt_x$ alloy.

alloys have layered structures ($L1_0$ and $L1_1$ types) and Ni is just before Cu in the periodic table. The composition dependence of diffuse intensity for Ni–Pt alloys is rather similar to that for Cu–Au alloys.

Acknowledgments

The authors would like to express their thanks to Dr Y Watanabe and the staff of the *sample preparation room of the Institute for Materials Research, Tohoku University,* for help in preparing one single-crystal ingot ($x = 0.50$).

References

Borie B and Sparks C J 1971 *Acta Crystallogr.* A **27** 198
Cadeville M C, Dahmani C E and Kern F 1986 *J. Magn. Magn. Mater.* **54–57** 1055
Dahmani C E, Cadeville M C and Bohnes V P 1985 *Acta Metall.* **33** 369
Klaiber F, Schönfeld B and Kostorz G 1987 *Acta Crystallogr.* A **43** 525
Kostorz G 1983 *Physical Metallurgy* 3rd edn (New York: North-Holland) p 793
Krivoglaz M A 1969 *The Theory of X-Ray and Thermal Neutron Scattering by Real Crystals* (New York: Plenum)
Moss S C 1969 *Phys. Rev. Lett.* **22** 1108
Moss S C and Clapp P C 1968 *Phys. Rev.* **171** 764
Ohshima K and Watanabe D 1973 *Acta Crystallogr.* A **29** 520
Pearson W B 1958 *A Handbook of Lattice Spacings and Structures of Metals and Alloys* (Oxford: Pergamon) p 782
Saha D K, Koga K and Ohshima K 1992 *J. Phys.: Condens. Matter* **4** 10093
Saha D K and Ohshima K 1993 *J. Phys.: Condens. Matter* **5** 4099
Saha D K, Ohshima K, Wey M Y, Mitda R and Kimoto T 1994 *Phys. Rev.* **49** 15715
Schönfeld B, Ice G E, Sparks C J, Haubold H G, Schweika W and Shaffer L B 1994 *Phys. Status Solidi* b **183** 79